Functionally-graded serrated fangs allow spiders to mechanically cut silk, carbon and Kevlar® fibres

Gabriele Gabriele[1,2*$] & Diego Misseroni[3$], Filippo Castellucci[4, 5], Nicolò G. Di Novo[2], Nicola M. Pugno[2, 6 *]

[1] Department of Animal Biosciences, Swedish University of Agricultural Sciences, 750 07 Uppsala, Sweden

[2] Laboratory for Bio-Inspired, Bionic, Nano, Meta, Materials & Mechanics, Department of Civil, Environmental and Mechanical Engineering, University of Trento, Via Mesiano, 77, 38123 Trento, Italy

[3] Laboratory for the Design of Reconfigurable Metamaterials & Structures, Department of Civil, Environmental and Mechanical Engineering, University of Trento, Via Mesiano, 77, 38123 Trento, Italy

[4]Department of Biological, Geological and Environmental Sciences—University of Bologna, via Selmi 3, 40126, Bologna, Italy

[5] Zoology Section, Natural History Museum of Denmark—University of Copenhagen, Universitetsparken 15, 2100, Copenhagen, Denmark

[6] School of Engineering and Materials Science, Queen Mary University of London, Mile End Road, London E1 4NS, UK

[$] These authors contributed equally

* Corresponding authors: gabriele.greco@slu.se; nicola.pugno@unitn.it;

Keywords: serration, cutting, spider silk, stress concentration, engineering, functional structures.

Author Contributions: Conceptualization: GG, NMP. Methodology: GG, DM, NDN, FC. Analytical model: NMP. Investigation: GG, DM, NDN, FC. Funding acquisition: GG, DM, NMP. Supervision: GG, NMP. Writing – original draft: GG, DM. Writing – review & editing: GG, DM, NDN, FC, NMP.

Competing Interest Statement: Authors declare that they have no competing interests.

Data availability statement: All the data used in this work are included in the manuscript and in the supplementary material.

Abstract

Before humans and allegedly any animal group, spiders developed “functionally graded toothed blades" that cut one of the toughest biological materials: silk. Here, we reveal the importance of micro-structured serrations in spiders’ fangs that allow these animals to cut silk and artificial high-performance fibres, such as carbon or Kevlar®. The importance of serrations revolves around the stress concentration at the interface between the fang and the fibres, resulting in a cutting efficiency superior to that of a razor blade. This efficiency is high also for fibres with different diameters like silk, because of the serration grading that allows a smart positioning of the fibre in the optimal cutting condition. We propose that when the silk fibre is grasped by the fang, it slides along the serrated edge till it gets locked in the serration with a comparable size, where the load to cut is minimal. Our results provide a new perspective on cutting mechanisms and set the roots for spider fang-inspired cutting tools.

Introduction

Pushed by the challenges imposed by nature, many animals have efficiently solved biological tasks by coupling fascinating morphological traits and behaviours. Among the creatures that inspire researchers, spiders sit in a bright spot. They are capable of efficiently detecting imperceptible air flows and vibrations to locate prey or a mate[1], from which some males can efficiently flee and avoid cannibalism using a catapult action that accelerates them up to 51g[2]. But above all, spiders are masters in spinning and weaving silks, gaining a special position in the minds of the intellectuals of every epoch[3]. Spiders can produce and spin several types of silk, which present different mechanical properties[4]. In particular, the strength and toughness of major ampullate silk, which outranks many natural and artificial fibres, have allowed these animals to fly to conquer many natural habitats and build robust orb webs[5]. In these, spiders outsource their acoustic sensors expanding their sound-sensitive surface area by about 10000 times[6]. Moreover, the capability of major ampullate silk to store elastic energy has allowed spiders to achieve performance otherwise impossible by using only their muscles. Recent works revealed how spiders can accelerate their body up to 80g[7] and lift prey 1000 times their body mass[8,9]. This very last work describes the interaction between the animals and the web, made of complex and disorganized networks of tough silk threads, which were promptly removed by the spider, if felt as impediments, by grasping them with the fangs and cutting.

The capacity to cut and handle silk lines is fundamental for spiders, especially for those that build webs[10]. Nonetheless, the cutting mechanism has yet to receive much attention. Many authors have limited themselves in observing that the silk lines are brought into the vicinity of the mouth and broken up[11]. Some authors propose that special digestive enzymes could be involved in the cutting process due to the impossibility of fangs to act like scissors[10,12–14]. This intuition agrees with what is commonly observed in orb weavers that ingest parts of their webs without apparent strong mechanical action of the mouth apparatus[10]. The movements and the morphology of the fangs themselves are not similar to those of scissors or snipping tools.

Nevertheless, spiders possess a tool, which has been surprisingly overlooked, that may be involved in the cutting of the silk lines, and that can justify alone an exclusive mechanical action: the micro-graded serration on the fangs. Interestingly, this particular trait of spiders has been repetitively observed in many families, but it has never been

associated with a specific function[15], even though Foelix[16] and Peters[17] hypothesized its involvement in cutting silk lines.
Serration on fangs and teeth is not only a spider's peculiarity but is also a distinctive characteristic of other animals, such as dinosaurs[18], crocodiles[19], and sharks[20]. Because of their mechanical efficiency, serrated blades, scissors, knives and swords were introduced by humans at the end of the XIX century to cut different materials (e.g. wood, steel) and food (e.g. bread, steaks). In particular, the serration in a blade is essential to efficiently cut compliant materials (such as silk), since a serrated edge can easily push its scallops into the material minimizing the required normal force[21].
Thus, to be an effective tool for cutting silk, the micro-serration on spiders' fangs should drastically reduce the force and time required to cut fibres, thus avoiding the need for gastric enzymes to break down silk.
In this work, different experimental techniques, including custom-made micromechanical and behavioural experiments, are combined with knowledge of the underlying mechanics and functional anatomy of spiders to understand the role of serration in the cutting process. Moreover, to better reveal and understand cutting mechanics and exclude the involvements of enzymes, we challenged the spiders to cut not only silk fibres, but also other high-performance materials, such as carbon or Kevlar® fibres.
Finally, finite element (FE) simulations were performed and an analytical model was developed to prove the mechanical efficiency of graded serration in reducing the required force to cut a fibre.
Our findings lead us to propose the following cutting mechanism. The silk fibre is grasped by a fang, causing it to slide along the serrated edge of the fang until it becomes locked and then broken down in a serration of similar size.
In summary, spiders can cut silk mechanically with their serrated fangs. It is no surprise that we found such a trait in 48 araneomorph families that produce major ampullate silk and thus benefit from a tool to handle such an extreme fibre. By explaining how spiders cut, we reveal a basic engineering principle that can inspire the design of highly efficient cutting tools.

Results and Discussion

In previous work, we documented *Steatoda* spp. spiders hunting larger prey by lifting using pre-tensioned silk lines[8,9]. When the spider is lifting the prey, the dense tangle of silk threads should impede its movements, reducing the efficiency of the process. However, this does not happen since the spider is able to cut the silk lines promptly. This cutting is demonstrated and recorded through a high-resolution, high-speed camera, showing how *spiders can cut silk threads in less than 0.1 s* (**Fig. 1**, Supporting Video S1). The claws bring the wire close to the mouth, and the fangs open with their tips facing the thread and grab it; after which the thread seems to slide on the fang and breaks down. The observed timing and phenomenology agree with what has already been documented in the literature[10–13]. The difficulties of having this phenomenon recorded at high magnification (for example, by using a microscope) handicaps its understanding, making it hard to state if some chemical action is involved.
For these reasons, to better understand the cutting mechanism, spiders should be forced to cut different fibres in terms of materials and diameters. In this sense, Kevlar® and carbon fibres are the best candidates since they are considered among the strongest and toughest artificial fibres. Moreover, these fibres are resistant to enzymes and chemical attacks, which is important to understand if a chemical action is involved in spider cutting.

Thus, man-crafted orb webs in Kevlar® were used to induce spider cutting (Fig. S1a,b) by inserting the animal in a terrarium with these artificial webs.
During the night, spiders were recorded cutting and destroying the Kevlar® threads in order to build their silk-web (Fig. S1c,d; Fig. S2a,b). In particular, the animals followed the usual process to build orb webs. First, they spun the frames of the silk structures[10]. Then, they removed the key structural threads in the artificial webs (Fig. S2,c). In contrast to what happens with silk, cutting the artificial fibers proved challenging for the spiders. Unlike silk, where threads are typically cut in a fraction of a second, the artificial threads required considerable effort to cut, >>10 s, likely involving the application of shear forces through fang movements (Supporting Video S2). (Supporting Video S2). Eventually, the artificial fibres were cut (Supporting Video S3), and the spiders constructed their web, using the leftovers of the artificial one as support (Fig. S2d,e).
At the same time, some other spiders were allowed to build the web in some supports where no artificial web was present. Then, some radial and spiral threads were removed and substituted with carbon fibres to stimulate spiders to also cut these artificial fibres. In a similar way to what has been described before, the animals removed the carbon fibres in the modified webs and promptly placed them at the edge of the webs. Then the animals filled the empty spaces with silk lines (Fig. S3).
After being cut by the spiders, the fibres' cutting surfaces were observed with Scanning Electron Microscopy. Interestingly, the fracture surfaces of the silk and carbon fibres cut by the spiders (Fig. S4a,b) were similar to those broken artificially using scissors or tensile tests (Fig. S5a-c). Conversely, in the case of Kevlar® fibres, an exhausted, and plasticized fracture surface was observed (Figs. S4c and S6). Plus, the fibres presented micro-damages along their length, suggesting that the spider did not cut easily the fibre (Fig. S4d).
Strong mechanical actions imply powerful muscles in the chelicerae apparatus to exert the load necessary to cut such challenging fibres. Since the force exerted by a muscle is proportional to its section, we can consider the muscles of the fang (with the smaller volume) to be the limiting factor of the paw-fang-paw system of constraint. To investigate the biomechanics of the fang and estimate the maximum force sustainable (F_s) by the muscles of the fangs in the closed position, we performed 3D μ-tomography. The results are depicted in Fig. S7 and Supplementary Video 4, which show that there is no separation between the fang and exoskeleton, which are connected through two flexible thickenings of the shell that determine the rotation axis. Five muscles can be identified, four flexors (white, red, violet and pink) and one extensor (blue). The tendons are anchored to the protrusions at the base of the fang.
It is very challenging to quantify the biomechanical muscle capabilities of spiders and to evaluate the forces acting on the fang apparatus[22], but a simplified calculation could still be conducted. Based on the geometrical parameters obtained from these 3D models (see Supplementary Section S1, Table S13), and considering the values of specific tension (force divided by the physiological cross-sectional area) of muscles of some arachnids obtained from literature[23,24], a force F_s between 17 and 27 mN has been estimated, which is enough to justify a pure mechanical action in silk cutting. Such a value is comparable with the biting forces of common insects and spiders of similar size[25–27].
However, from the behavioural experiments, we observed that (i) the estimated force that a single fang can exert may not be enough to cut fibres such as Kevlar® or carbon and (ii) the transversal displacement applied to the silk thread is small (see Supporting Video 1). Thus, spiders should own other structural features that enhance their cutting efficiency, thus reducing both the maximal force and displacement required to break the fibres. To

understand this, two kinds of experiments were performed on natural (silk) and artificial (Kevlar® and carbon) fibres (**Fig. 2**). The first type of experiment is a standard tensile test. These tests provided us with the mechanical properties of tested materials (Fig. S7, Tables S1-S3), as well as their average failure loads (Fig. 2e-g, left bars). The second type of experiment was performed using a customised micromechanical experimental setup designed to mimic the spider's cutting process. Such setup resembles a sort of 3-points test that hereafter we call a “cutting experiment” (see Materials and Methods section). Through these experiments, we estimated the fibres breaking load (Fig. 2e-g, middle and right bars), and the corresponding deflection angles (or displacement) at break. With these quantities, it was possible to calculate the stress arising within the fibres (Fig. S10, and S11; Tables S4-S12).

The results presented in Fig. 2e-g show that the fangs are significantly more efficient than a razor blade in cutting the fibres. This difference can be ascribed to the presence of a micro-serration on the fang since the radii of curvature of the razor blade and fang are similar. Indeed, the presence or the absence of a micro-serration is the main difference between the fang and the razor blade, respectively (Fig. S8). This fact implies that spiders are favoured by owning serrated fangs when cutting silk is required, in agreement with what was proposed by Peters[17] and Foelix[16]. Furthermore, from Fig. 2e-g it is clear that the maximal force that spiders can exert, highlighted with a red band in the graphs, is enough to mechanically cut both carbon and silk fibres, but apparently not to cut Kevlar®**.**

Contrary to what happens for crocodiles, sharks, and *Tyrannosaurus*[18–20], spider fang serration is not homogeneously spaced (Fig. S12). Although the mechanical response of the fibre to such serration depends on its geometry (see later), the previously presented micromechanical customized setup cannot precisely control the relative position of the fibre with respect to the serration (Fig. S13). This explains why the average values of cutting forces obtained with the mechanical tests are still too high to fully justify the mechanical cutting of Kevlar® fibres by spiders, given the limitation on the maximum force that fang muscles can exert. However, note that multiple cuttings remain a plausible option for the spider.

Systematic numerical simulations were performed to better understand the silk cutting mechanism adopted by spiders and the role played by serrations (see Materials and Methods section for further details). **Fig. 3** highlights the pivotal role of serrations in the cutting process. When a fibre is pressed onto the fang, stress concentration is induced by the two bulges at the top of the serration (Fig. 3a-b). This stress concentration initiates crack propagation, leading to the failure of the fibre. The numerical simulation results (Fig. S14) illustrate the impact of serrations on the cutting process. By subjecting the fibre pressed on the serrated fang to a consistent transversal displacement of 0.50 mm, the area within the fibre experiencing von-Mises stress exceeding 326 MPa, i.e., strength obtained from tensile tests (Table S1), is maximized in cases $a/R \sim 1$. It is noteworthy that in scenarios when $a/R \gg 1$ no point within the fibre surpasses 326 MPa. To further investigate the role of serration in silk cutting, we have fixed the area where the von-Mises stress is higher than 326 MPa and we measure the load necessary to achieve this value. The results (Table S14) indicate that the load required to break the fibre is reduced by 80% when $a/R=0.96$. These results strongly suggest that the optimal cutting condition is the one when the fibre and the serration have comparable dimensions.

In addition to numerical simulations, cutting mechanics can also be interpreted and explained with an analytical model (see section S2, Fig. S15). This considers how the serration, friction, and pretension applied by the spider on the fibre modulate cutting efficiency, here defined as

$$Cutting\ efficiency = 1 - \frac{P_{ST}}{P_0} = \left(1 - \frac{\sigma_T^2}{\sigma_c^2}\right)^{\frac{3}{2}} \left(\sqrt{1 - \left(\frac{a}{R}\right)^2} + \mu \frac{a}{R}\right) \quad (1)$$

where P_{ST} is the load to cut the fibre with serration (P_S if only with the serration) and a pre-tension (P_T if only with the pre-tension) and P_0 is the critical load necessary to cut the fibre in the absence of serration and pre-tension, here defined as control condition of negligible cutting efficiency. The critical stress σ_c and the pre-tension stress σ_T are defined in supplementary section S2. If the cutting efficiency is positive the cutting is aided, by either the serration or the pre-tension. The effect of serration is ruled by the ratio *a/R* and by the friction coefficient μ between the fang and the fibre. If cutting efficiency is negative, it means that the load required to cut the fibre is higher than P_0, meaning that the condition is disadvantageous for cutting. The results predicted from the theoretical model are depicted in **Fig. 4** (see supplementary section S2 for more details on the construction of the model) and have been obtained using the experimental data reported in this work. From Figure 4a is clear that the condition necessary to have an optimal cutting due to serration is *a/R* close to 1. In particular, for $\mu=0.3,\ 0.5$ the load to break the fibre in the presence of serration is reduced by a factor of 56%, and 36% respectively. In general, serration has a positive effect on cutting when $a/R>0.54$ for $\mu=0.3$ or $a/R>0.8$ for $\mu=0.5$, suggesting that the lower the friction the sooner and the higher the positive effect of serration. Additional aid in cutting silk lines may be provided by additional tension in the fibres induced by the spiders by pulling with the legs the threads[28], as it is commonly found in cutting-leaf ants that prior to the cutting stiffens the leaves by means of vibrations[29]. Figure 4b shows the effect of pre-tension on cutting efficiency, and it is clear that having a pre-tension on the fibre always positively affects cutting efficiency. In particular, when $\frac{\sigma_T}{\sigma_c} = \frac{1}{2}$ the cutting efficiency is about 40%. A combined effect of pre-tension and serration is displayed in Figure 4c, from which with a ratio $a/R=0.84$ we obtain a cutting efficiency of 30% in the absence of pre-tension, which can raise up to 50% by applying a pre-tension of $\frac{\sigma_T}{\sigma_c} = 0.45$. Overall, the analytical model aligns well with the numerical simulations' results, i.e., the optimal cutting condition is achieved when the fibre and the serration have comparable size.

The cutting phenomenon cannot be visualized in focus using light microscopy, which underscores the importance of the proposed model (SS2) and the numerical simulations in providing a potential explanation. We propose that the cutting is achieved by smart positioning the fibre to be cut along the serrated edge of the fang. Thanks to the graded serration of the spider fang and its curvature, the optimal cutting condition could be achieved just by the fibre sliding on the fang (Figure 4d,e). Thus, during cutting, the fang grasps the fibre that slides on the different serrated edges till it gets locked in the one with comparable size and thus where the cutting load is nearly minimal. This means that the presence of a functionally graded spacing between subsequent serrations (contrary to other animals[18,19,21]) permits the cutting of multiple fibres with different dimensions (such as those found in the silk threads spun by spiders). Both these aspects imply that serration is an advantageous trait for spiders and should be commonly found in these animals.

A closer look at the literature data and original data indicates that serration has been observed in 48 araneomorph families and at least three mygalomorph families[30] (Figs. S16-17, supplementary data sheet). This means that the serration may have played a

function even in the absence of major ampullate silk (e.g. aiding the chewing and smashing of prey). Thus, the role of serration in cutting the tough major ampullate silk may have been later acquired in Araneomorphae[31].
The results reported in this article highlight that the sole mechanical action produced by spiders with their serrated fangs could be enough for cutting silk, carbon and even Kevlar® fibres. Enzymes and gastric fluids may play a role in cutting mechanics, as suggested by Eberhard[14], though this does not rule out the mechanical involvement of fang serrations. Spider gastric fluids, while typically unable to rapidly dissolve major ampullate silk, are unlikely to solely induce fast cutting observed (~0.1 s)[32,33]. Additionally, such chemical action would not significantly affect Kevlar® and carbon fibers, which spiders also cut. Thus, it remains possible that chemical enzymes weaken the fibres, but it is sure that the mechanical action that cuts them, as here demonstrated.
Finally, Fig. 2 clearly demonstrates that serrated blades are more effective than non-serrated blades in cutting high-performance fibres like Kevlar® and carbon. With the ongoing advancement of high-performance fibres that exhibit toughness and strength comparable to native silk[34–36], we believe our findings offer valuable insights and lay the foundation for the development of spider fang-inspired cutting tools designed to efficiently cut fibres of varying diameters.

Conclusions

Our understanding of the mechanisms that occur in nature is challenged by the complexity of the systems involved and technical limitations. Among the most captivating and understudied natural phenomena, the cutting of silk lines performed by spiders keeps awake the minds of both arachnologists and engineers. This work shows that spiders are efficiently capable of mechanically cutting silk and other highly performant artificial fibres, such as carbon and Kevlar® fibres. These were selected to challenge the spiders and to better reveal and explain the cutting mechanism. By combining experimental, theoretical, numerical and biological approaches, we provide evidence that the cutting of silk lines is mechanically possible due to the presence of functionally graded fang serrations that could also allow fibre smart positioning before optimal cutting. Although this does not exclude the involvement of gastric enzymes in this phenomenon, it surely gives a solid reason for the pervasive distribution of fang serration among spiders. Here, we suggest that such a micro-structured serration has secondarily acquired a cutting function as a morphological tool to optimize cutting mechanics by reducing the forces necessary to break up silk fibres.

Materials and Methods

Spiders and silk extraction

The spiders under study are the common orb-weaver *Nuctenea umbratica* (for the interaction with artificial webs) and the tangle web spider *Steatoda triangulosa* (for the interaction with the natural web). Adult specimens were collected around the campus in Trento (Italy) and used in the cutting experiments. The silk was forcibly extracted from *N. umbratica* at ~1 cm/s. *Nuctenea umbratica* was selected because it is known to build orb webs in captivity under certain environmental conditions, i.e. the presence of at least three rigid stick-like supports. Man-crafted orb webs in Kevlar® were built using polystyrene supports (Figure S1a,b) to induce spiders to cut artificial fibres. The spiders were then let inside the cage and monitored with a nocturnal vision camera during the night. At the same time, some other spiders were allowed to build the web in some supports where no artificial web was present. Then, some radial and spiral threads were removed and substituted with carbon fibres to stimulate spiders to cut these artificial fibres. In the case of experiments on spiders, according to Italian regulations on animal protection and EU Directive 2010/63/EU for animal experiments, we are not required to obtain ethical approval.

Artificial spider webs

The artificial orb webs were produced with the support of a styrofoam base, from which 8 pillars were placed to elevate the web from the plane. Kevlar® Technora T240_440dtex (Teijin) and Carbon C T24-5.0/270-E100 (SGL) fibres were used to create the main frame and the spirals. Then, the artificial fibres were glued on the frame by Super Attack glue droplets.

High-speed video

A Sony PXW-FS5 equipped with Nikon AF Zoom-Micro-Nikkor 70–180 mm f/4.5–5.6 D ED lens was used to record high-speed cutting videos. These movies were recorded at a frame rate of 240 fps (24p).

Cutting experiments with spiders

In a glass terrarium (30x30x40 cm^3) the artificial orb web structures were placed and subsequentially a small refuge was created using rolled paper. This was placed in a high corner of the cage, to provide to the spider during the day. The spider was then placed in the terrarium and recorded at night with the support of a high-resolution Sony Camera with night visual (Sony FDR-AX700 4K).

Scanning electron microscopy (SEM)

We used a FE-SEM Zeiss Supra-40/40VP to perform SEM microscopy. The samples were coated by using a Quorum machine T150 with the Pt/Pd 80:20 program in a reduced argon atmosphere. SEM images were used to measure serration spacing *c* used to define the initial crack length *a* in Equation (1) and reported in Figure S5 (right). Such values were evaluated by computing the averages and the standard deviation of several measurements conducted on different specimens.

Mechanical tests

Two kinds of experiments were performed on natural and artificial fibres. Such experiments were performed using two loading frame machines: a nano-tensile Agilent UTM T150 and a mu-strain by Messphysic. The use of two different machines was dictated by (i) the expected loads to be applied to break the different fibres (i.e. higher load for Kevlar®) and (ii) space constraints. For instance, the needle-cutting experiments were impossible with the nano-tensile machine since there was insufficient space to mount the razor blade on its upper grip. Before the execution of the experiments reported in this article, preliminary tests were performed with both machines to verify the correspondence of the collected results. In both experiments, the samples were prepared as follows. Paper frames were obtained by cutting a square window (10x10 mm^2) and placing double-sided tape to attach the fibres. For spider silk, no extra glue was necessary, whereas, for carbon and Kevlar® fibres, we also used super glue to fix the fibres better. In all the cases, the fibres were mounted with a bit of slack to ensure minimal pre-stress. The diameter of the fibres (used to calculate the cross-sectional area and thus the stress) was measured before the experiments with the support of an optical microscope at five points for each fibre and then averaged. The results are reported in supplementary tables S1-10.

Tensile experiments. These experiments were performed to estimate the mechanical properties of the fibres. We used the nanotensile machine to test silk and carbon fibres, while a mu-strain (by Messphysic) to test Kevlar® fibres. The imposed test speed (displacement gauge machines) was 6 mm/min in all the mechanical tests. The nominal stress and strain were calculated, respectively, by dividing the force by the initial cross-sectional area and the imposed displacement by the initial gauge length (taking into account the slack before the initial loading). Young's modulus was obtained by linear fitting of the initial linear elastic region of the stress-strain curve, strength as maximal stress, ultimate strain as maximal stain and toughness modulus as the area under the nominal stress and strain curve.

Cutting experiments. These experiments were specifically designed to mimic the cutting mechanism used by spiders. The test is a sort of 3-points test, where the fibres are fixed at their ends and loaded transversally with the loading machine. The setup consisted of a loading frame machine (Figure 3a) whose upper grip, the one connected with the load cell, holds different cutting elements. These were a needle (0.2 mm diameter, Figure 3b), a razor blade (Surgical Scalpel blade #10, Figure 3c), and a spider fang (glued on a steel support, Figure 3d) from an adult specimen of *Nuctenea umbratica*. For the fang, in particular, we ensured that the serration was pointing upwards against the fibre. The needle was selected to have a diameter comparable to the middle part of the fang. The razor blade was selected to have a cutting edge as sharp as the one of the spider fangs (curvature radius 3.5 μm, Figure S8), with the sole main difference of not having a serration. These experiments were performed for the major ampullate silk of an adult *Nuctenea umbratica*, carbon fibres and Kevlar® fibres. During the execution of the experiments, the machine applied a strain (test speed of 6 mm/min) and recorded the applied load until the failure of the fibres. We used the nanotensile machine to perform the cutting tests with the needle and the fang on silk and carbon fibres. We used the mu-strain to test (i) silk and carbon fibres with the razor blade and (ii) Kevlar® fibres with all three different cutting elements. The cutting loads estimated using the three different cutting elements (needle, razor blade, and fang) were compared to those obtained via standard tensile test (4 types of test in total).

Tomography of the teeth

We undertook microtomographic imaging of the spider fangs in the TOMCAT beamline of the Swiss Light Source[37]. The used energy was 21 keV, and the distance detector-spider was 20 cm. This was euthanized in alcohol at 70% and kept in a vial to guarantee adequate contrast. The images were pre-elaborated with ImageJ software[38] using the plug-in "WEKA trainable segmentation" to classify the grey-scale images into different classes. The segmentation and the 3D volumes were measured with the support of 3DSlicer, with which all the volume images were produced[39].

Simulations

We performed systematic Abaqus (Static, General) simulations to investigate the role played by the functionally graded serration in the cutting mechanism adopted by spiders.

The silk fibers were modelled as 3D elements with Young's modulus and diameter, respectively, E=7 GPa and d=3.33 μm. Six different simulations were performed, one for each of the serration spacing $c=\{1.6, 3.292, 4.782, 6.012, 8.643, 9.514\}$ μm (Figure S12). The radius of curvature of the contact region r and the distance between the contact points (2a) are assumed to be r=0.25*c. To reduce computational costs, we divided the fibres into two main regions to have a finer mesh only where necessary. The two parts were joined together using a tie constraint. In the external regions, we used a coarser mesh made of C3D10 elements (10-node quadratic tetrahedron) with a maximum size of 0.5. Conversely, the central region was discretized by a much finer mesh made of C3D10 elements (10-node quadratic tetrahedron) with a maximum size of 0.035. The refinement in the central region is essential in correctly estimating the stress concentration arising at the contact region between the fiber and the fang. A mesh-sensitive study was performed to estimate the optimal mesh sizes that led to mesh-independent results.

To better compare the real experiments, we tried to replicate the actual fang using the SEM images as a template. Such 3D objects were realized parametrically in *SolidWorks* and then imported into Abaqus for running the simulations. Since the geometry of the serration fangs used in the simulation is an approximation of the real geometry, the simulation results provide just an indication of the stress concentration induced by serrations in the fibers. The final results are shown in Figure 3 and Table S14. The fangs were modelled as 3D elements with Young's modulus E=10 GPa[40–42] and meshed with C3D4 elements (4-node linear tetrahedron). To obtain reasonable results and to avoid convergence issues, we reduced the mesh size to 0.01 in the vicinity of the serration, namely in the area where contact with the fibers happens.

The contact fiber-fang was modelled using a surface-to-surface frictional algorithm (friction coefficient 0.3). We have assigned the master and the slave roles to the fang and the fiber surfaces, respectively. In the simulations, the fibers were constrained with two hinges at the two ends, while a constant displacement was imposed on the fang to mimic the setup of the cutting experiment. By virtue of the remarkable ductile properties exhibited by silk fibres, we have opted to employ the von-Mises stress as a criterion for assessing failure, which is a common approach used for both fragile and compliant materials[43,44].

<u>Mapping of serration on the spider tree of life</u>

Information regarding spider taxa for which fang serration is present was acquired by direct observation of spider specimens and by screening literature data. The presence of serration was plotted on a cladogram including all major spider groupings derived from the phylogenomic work by Kallal et al.[45]. The explored literature was[16,30,46–52]. A list of spider taxa for which serration is reported in the bibliography, together with novel data obtained in this work is reported in the Excel® supplementary data.

Data obtained from[15,16,52,30,45–51].

<u>Statistical analysis</u>

To analyse the data obtained from the experiments we employed one-way ANOVA. For each type of experiment, the sample size was between 9 and 22. No outliers were excluded from the analysis. The p-value was calculated using the data analysis package in Excel®.

Acknowledgments

We acknowledge the Paul Scherrer Institut, Villigen, Switzerland for provision of synchrotron radiation beamtime at beamline TOMCAT of the SLS and would like to thank Dr. Schlepütz Christian Matthias for assistance. G.G. and N.M.P. would like to thank the students Mattia Cipriani and Andrea Fiorese for their initial help in building the artificial orb webs, and the student Flavia Coluccia for the initial help in preparing the samples. N.M.P. and G.G. thank Prof. Antonella Motta for the help with Scanning Electron Microscopy facility. The authors acknowledge Prof. Jason Bond for the SEM image of *Ummidia*. G.G. and F.C. were supported by Aracnofilia – Italian Association of Arachnology. **Funding:** N.M.P. is supported by the Italian Ministry of Education, University and Research (MIUR) under the PRIN-20177TTP3S grants. D.M. is supported by the European Union project HE ERC-2022-COG-101086644-SFOAM. G.G. was supported by Caritro Foundation (prot. U1277.2020/SG.1130) and is supported by the project "EPASS" under the HORIZON TMA MSCA Postdoctoral Fellowships - European Fellowships (project number 101103616).

References

1. Young, S. L. *et al.* A spider ' s biological vibration filter : Micromechanical characteristics of a biomaterial surface. *Acta Biomater.* **10**, 4832–4842 (2014).

2. Zhang, S. *et al.* Male spiders avoid sexual cannibalism with a catapult mechanism. *Curr. Biol.* **32**, R354–R355 (2022).

3. Greco, G., Mastellari, V., Holland, C. & Pugno, N. M. Comparing Modern and Classical Perspectives on Spider Silks and Webs. *Perspect. Sci.* **29**, 133–156 (2021).

4. Arakawa, K. *et al.* 1000 spider silkomes : Linking sequences to silk physical properties. *Sci. Adv.* **6043**, 1–14 (2022).

5. Cranford, S. W., Tarakanova, A., Pugno, N. M. & Buehler, M. J. Nonlinear material behaviour of spider silk yields robust webs. *Nature* **482**, 72–76 (2012).

6. Zhou, J. *et al.* Outsourced hearing in an orb-weaving spider that uses its web as an auditory sensor. *Proc. Natl. Acad. Sci.* **119**, 1–7 (2022).

7. Han, S. I., Astley, H. C., Maksuta, D. D. & Blackledge, T. A. External power amplification drives prey capture in a spider web. *PNAS* **116**, 12060–12065 (2019).

8. Pugno, N. M. Spider weight dragging and lifting mechanics. *Meccanica* **53**, 1105–1114 (2018).

9. Greco, G. & Pugno, N. M. How spiders hunt heavy prey: The tangle web as a pulley and spider's lifting mechanics observed and quantified in the laboratory. *J. R. Soc. Interface* **18**, (2021).

10. Eberhard, W. *Spider Webs: Behavior, Function, and Evolution*. (The University of Chicago Press, 2020).

11. Barrantes, G., Zuniga-Madrigal, J. & Solano-Brenes, D. Hub thread removal behaviour in the orb weaver Leucauge mariana (Araneae: Tetragnathidae). *Arachnology* **18**, 517–520 (2020).

12. Tillinghast, E. K. & Kavanagh, E. J. The alkaline proteases of Argiope and their possible role in web digestion. *J. Exp. Zool.* **202**, 213–222 (1977).

13. Tillinghast, E. K. & Townley, M. A. Chemistry, physical properties, and synthesis of araneidae orb webs. in *Ecophysiology of Spiders* 203–210 (1987).

14. Eberhard, W. G. Small details in a large spider : cheliceral and spinneret behavior when Trichonephila clavipes (Araneae : Araneidae) cuts lines and wraps prey. *J. Arachnol.* **49**, 384–388 (2021).

15. Griswold, C. E., Ramirez, M. J., Coddington, J. A. & Platnick, N. I. Atlas of Phylogenetic Data for Entelegyne Spiders (Araneae: Araneomorphae: Entelegynae) with Comments on Their Phylogeny. in *Proceedings of the California Academy of Sciences* Volume 56, 1-324 (2005).

16. Foelix, R. F. & Erb, B. Microscopical studies on exuviae of the jumping spider Phidippus regius. *Peckhamia* **90.1**, 1–15 (2011).

17. Peters, V. H. Wie Spinnen der Familie Uloboridae ihre Beute einspinnen und verzehren. *Verh. naturwiss. Ver. Hambg.* **25**, 147–167 (1982).

18. Brink, K. S. *et al.* Developmental and evolutionary novelty in the serrated teeth of theropod dinosaurs. *Sci. Rep.* 1–12 (2015) doi:10.1038/srep12338.

19. Legasa, O., Buscalioni, A. D. & Gasparini, Z. The serrated teeth of Sebecus and the iberoccitanian crocodile, a morphological and ultrastructural comparison. *Stud. Geol. Salmant.* **29**, 127–144 (1993).

20. Moyer, J. K. & Bemis, W. E. Shark teeth as edged weapons : serrated teeth of three species of selachians. *Zoology* **120**, 101–109 (2017).

21. Frazzetta, T. H. The mechanics of cutting and the form of shark teeth (Chondrichthyes, Elasmobranchii). *Zoomorphology* **108**, 93–107 (1988).

22. Kallal, R. J. & Wood, H. M. High-Density Three - Dimensional Morphometric Analyses Reveal Predation - Based Disparity and Evolutionary Modularity in Spider ' Jaws '. *Evol. Biol.* **49**, 1–14 (2022).

23. Van Der Meijden, A., Langer, F., Boistel, R., Vagovic, P. & Heethoff, M. Functional morphology and bite performance of raptorial chelicerae of camel spiders (Solifugae). *J. Exp. Biol.* **215**, 3411–3418 (2012).

24. Heethoff, M. & Koerner, L. Small but powerful: The oribatid mite Archegozetes longisetosus Aoki (Acari, Oribatida) produces disproportionately high forces. *J. Exp. Biol.* **210**, 3036–3042 (2007).

25. Ruehr, P. T., Edel, C., Frenzel, M. & Blanke, A. A bite force database of 654 insect species. *bioRxiv* 2022.01.21.477193 (2022).

26. Patek, S. N., Baio, J. E., Fisher, B. L. & Suarez, A. V. Multifunctionality and mechanical origins: Ballistic jaw propulsion in trap-jaw ants. *Proc. Natl. Acad. Sci. U. S. A.* **103**, 12787–12792 (2006).

27. Wood, H. M., Parkinson, D. Y., Griswold, C. E., Gillespie, R. G. & Elias, D. O. Repeated Evolution of Power-Amplified Predatory Strikes in Trap-Jaw Spiders. *Curr. Biol.* **26**, 1057–1061 (2016).

28. Andserson, T. L. *Fracture Mechanics - Foundamentals and Applications*. (Taylor & Francis, 2005).

29. Schofield, R. M. S., Emmett, K. D., Niedbala, J. C. & Nesson, M. H. Leaf-cutter ants with worn mandibles cut half as fast, spend twice the energy, and tend to carry instead of cut. *Behav. Ecol. Sociobiol.* **65**, 969–982 (2011).

30. Raven, R. J. The spider infraorder Mygalomorphae (Araneae): cladistics and systematics. *Bull. Am. Museum Nat. Hist.* **182**, 1–180 (1985).

31. Gould, S. J. & Vrba, E. S. Exaptation—a Missing Term in the Science of Form. *Paleobiology* **8**, 4–15 (1982).

32. Walter, A. *et al.* Characterisation of protein families in spider digestive fluids and their role in extra-oral digestion. *BMC Genomics* **18**, 1–13 (2017).

33. Shao, Z., Young, R. J. & Vollrath, F. The effect of solvents on spider silk studied by mechanical testing and single-fibre Raman spectroscopy. *Int. J. Biol. Macromol.* **24**, 295–300 (1999).

34. Schmuck, B. *et al.* Strategies for Making High-Performance Artificial Spider Silk Fibers. *Adv. Funct. Mater.* (2023) doi:10.1002/adfm.202305040.

35. Xiao, Y. *et al.* Strong and Tough Biofibers Designed by Dual Crosslinking for Sutures. *Adv. Funct. Mater.* **34**, (2024).

36. Xiao, Y. *et al.* Bioinspired Strong and Tough Organic–Inorganic Hybrid Fibers. *small Struct.* **4**, (2023).

37. Stampanoni, M. *et al.* Tomographic Hard X-ray Phase Contrast Micro- and Nano-imaging at TOMCAT. *6th Int. Conf. Med. Appl. synchrotron radiation, Melbourne, Aust.* 13–17 (2010).

38. Schneider, C. A., Rasband, W. S. & Eliceri, K. W. NIH Image to ImageJ: 25 years of image analysis. *Nat. Methods* **9**, 671–675 (2012).

39. Fedorov, A. *et al.* 3D Slicer as an image computing platform for the Quantitative Imaging Network. *Magn. Reson. Imaging* **30**, 1323–1341 (2012).

40. Residori, S., Greco, G. & Pugno, N. M. The mechanical characterization of the legs, fangs, and prosoma in the spider Harpactira curvipes (Pocock 1897). *Sci. Rep.* **12**, 1–11 (2022).

41. Bar-On, B., Barth, F. G., Fratzl, P. & Politi, Y. Multiscale structural gradients

enhance the biomechanical functionality of the spider fang. *Nat. Commun.* **5**, 1–8 (2014).

42. Politi, Y. *et al.* A spider's fang: How to design an injection needle using chitin-based composite material. *Adv. Funct. Mater.* **22**, 2519–2528 (2012).

43. Akira, K. & Bosi, F. Nanographitic coating enables hydrophobicity in lightweight and strong microarchitected carbon. *Commun. Mater.* **1**, 72 (2020).

44. Wang, Y., Zhang, X., Li, Z., Gao, H. & Li, X. Achieving the theoretical limit of strength in shell-based carbon nanolattices. *Proc. Natl. Acad. Sci.* **139**, e2119536119 (2022).

45. Kallal, R. J. *et al.* Converging on the orb: denser taxon sampling elucidates spider phylogeny and new analytical methods support repeated evolution of the orb web. *Cladistics* **37**, 298–316 (2021).

46. Agnarsson, I. Morphological phylogeny of cobweb spiders and their relatives (Araneae, Araneoidea, Theridiidae). *Zool. J. Linn. Soc.* **141**, 447–626 (2004).

47. Moon, M. J. & Yu, M. H. Fine structure of the chelicera in the spider Nephila clavata. *Entomol. Res.* **37**, 167–172 (2007).

48. Ramìrez, M. J. The Morphology and Phylogeny of Dionychan Spiders (Araneae: Araneomorphae). *Bullettin Am. Museum Nat. Hist.* **390**, (2014).

49. Salvatierra, L., Brescovit, A. D. & Tourinho, A. L. Description of two new species of Tangaroa Lehtinen 1967 (Arachnida: Araneae: Uloboridae). *J. Arachnol.* **43**, 331–341 (2015).

50. Giroti, A. M. & Brescovit, A. D. *The taxonomy of the American Ariadna Audouin (Araneae: Synspermiata: Segestriidae)*. *Zootaxa* vol. 4400 (2018).

51. Lin, Y. *et al.* Asianopis gen. Nov., a new genus of the spider family deinopidae from Asia. *Zookeys* **2020**, 67–99 (2020).

52. Foelix, R. *Biology of Spider*. *Oxford University Press* vol. 53 (2011).

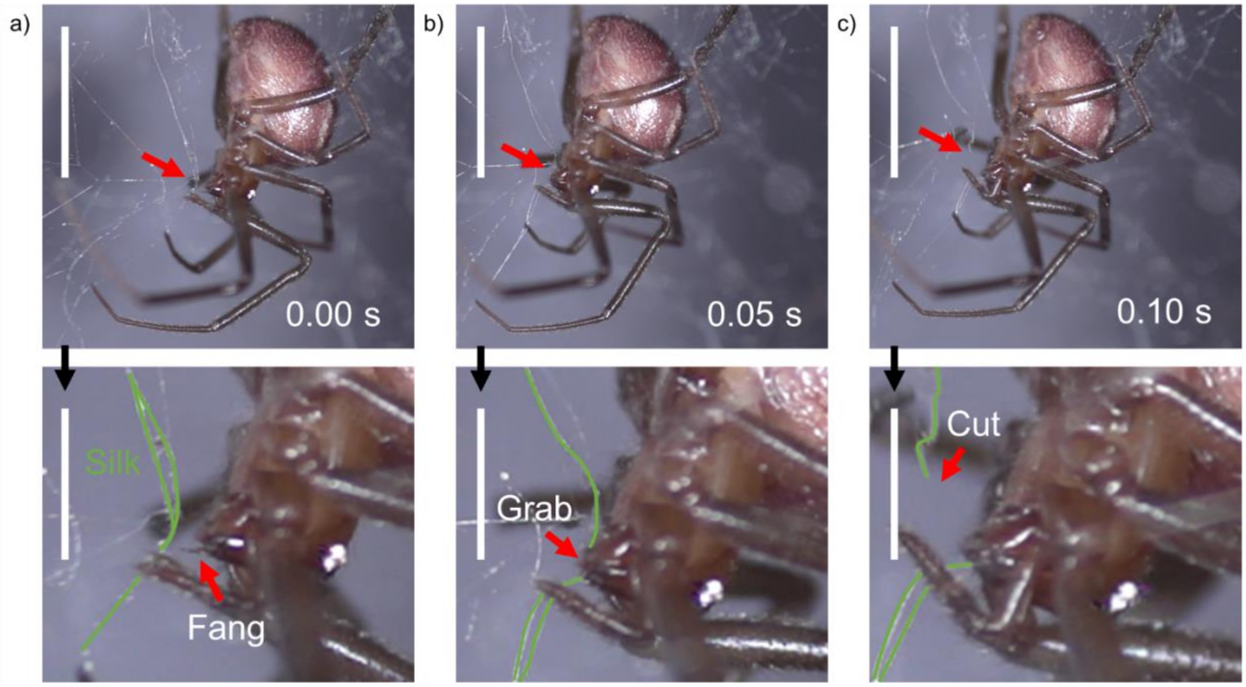

Figure 1. The cutting of silk by spiders. High-speed photograph of the silk cutting sequence in a female of *Steatoda* sp. a) The spider first grabs the silk lines (here highlighted in green) with the fang to subsequently b) squeeze them between the fang and the basal part of the chelicerae to c) cut them. Scale bars of 5 mm. The panels in the lower row are enlarged about three times and the relative scale bar is 12 mm.

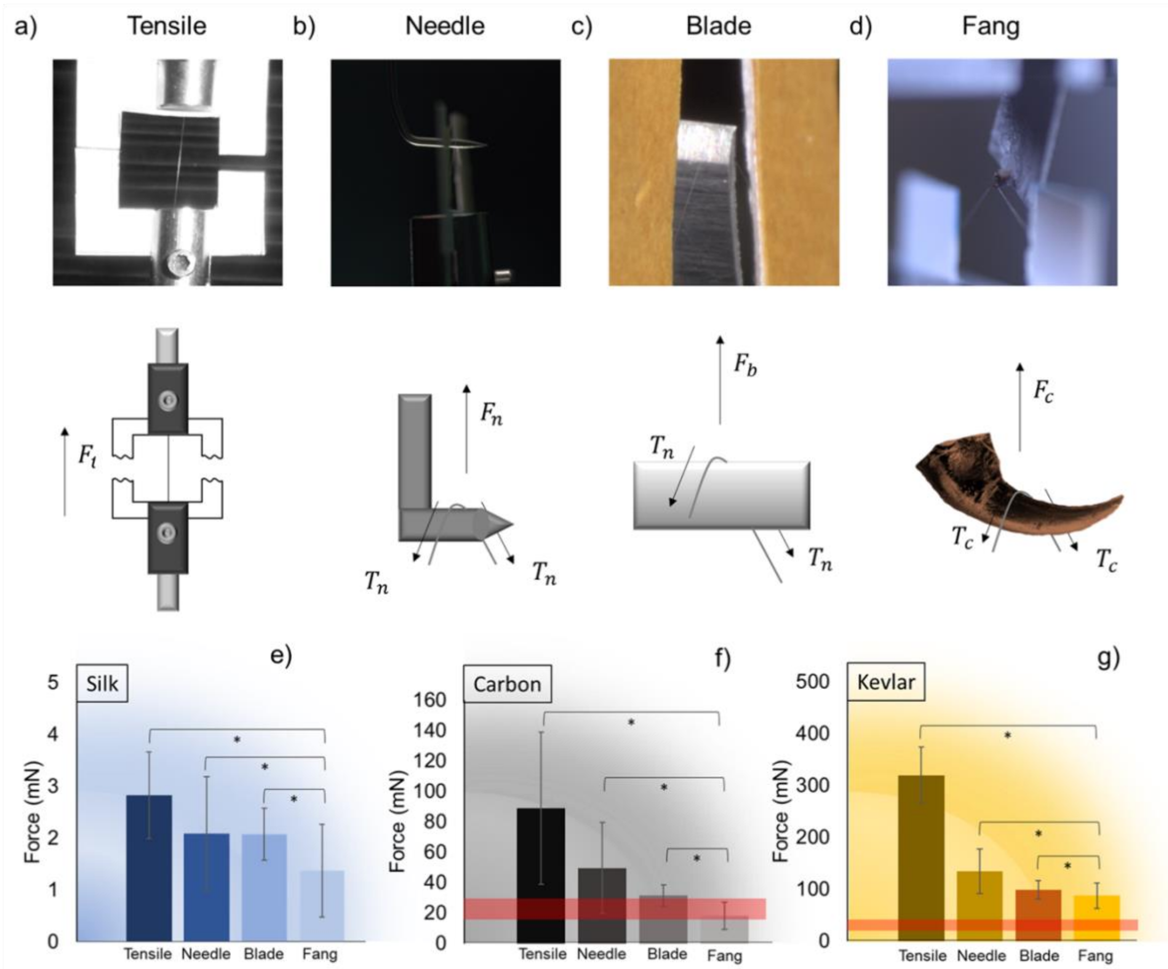

Figure 2. Micro-tensile or custom-made micro-cutting experiments. Experiments performed to evaluate the mechanical parameters to cut the fibres. a) Tensile tests, b) 3-points needle tests, c) 3-points blade tests, and d) 3-points fang tests. e) Force measured by the machine to cut silk lines with the previously mentioned setup. f) Force measured by the machine in order to cut carbon fibres with the previously mentioned setups. g) Force measured by the machine to cut Kevlar® fibres with the previously mentioned setups. The red horizontal bands in subfigures f) and g) represent the range of the maximal force exerted by the spider fang computed by means of computer tomography. In the silk panel, this maximal force (17-27 mN) has not been inserted because the forces in play are much lower than it. Stars indicate that the difference is significative with p-value<0.05. The sample size for each experiment was between 9 to 22 and the analysis was performed using Excel®.

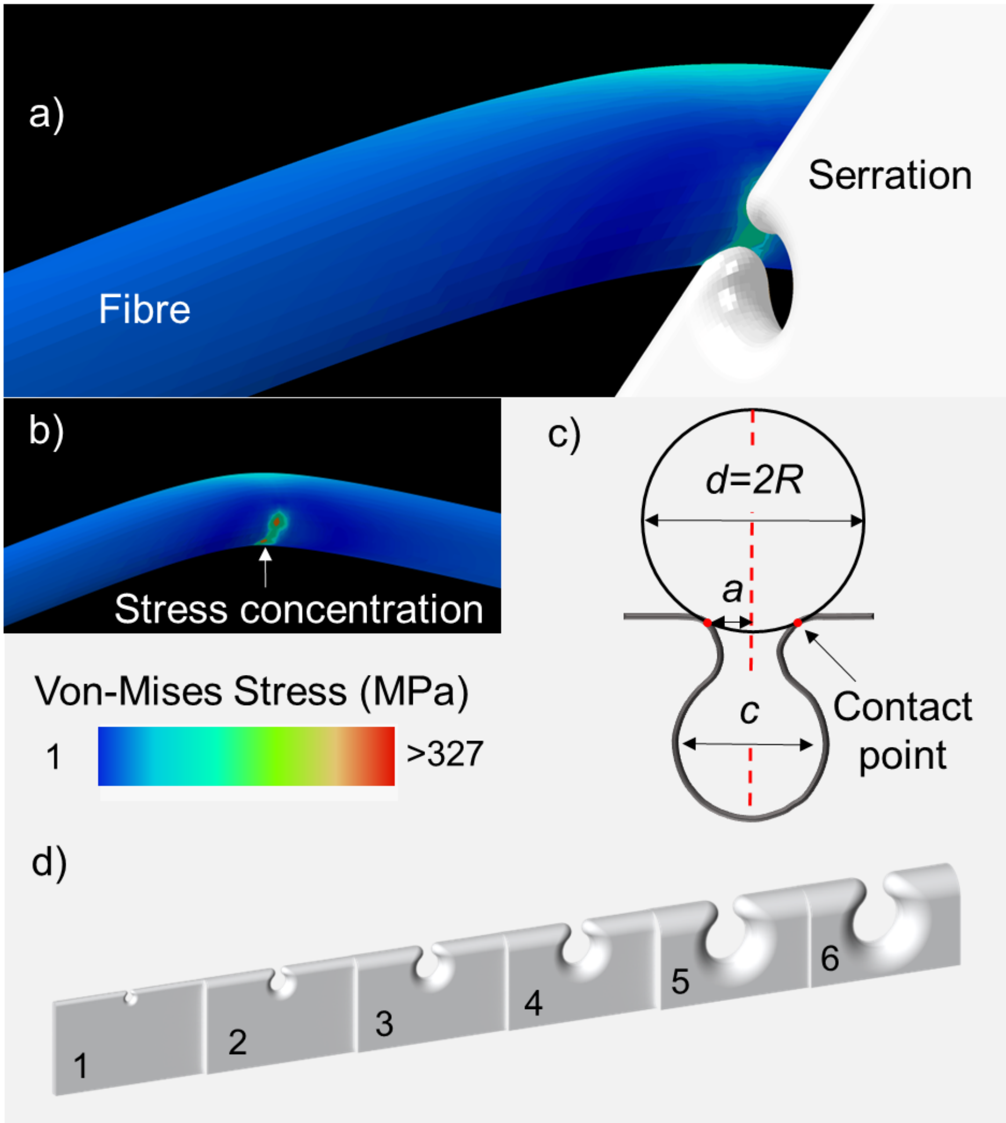

Figure 3. The serrations concentrate the stress at the interface between the spider fang and the fibre and improve cutting efficiency. a) Representative image of a simulation with the modelled serration used to cut the fibre. In this case *c=1.6*. b) The same image without the serration, which depicts the stress amplification in the contact point induced by the two upper serration bulges. c) Schematic of the main geometrical parameters involved in the modelling: fibre diameter (d), distance between the two contact points and thus also estimation of the spacing length (*2a*), and distance between serrations (c) considered to be proportional to the radius of the contact region. d) 3D model of the serration with the six different considered distances c in the serrations that are identified by the numbers.

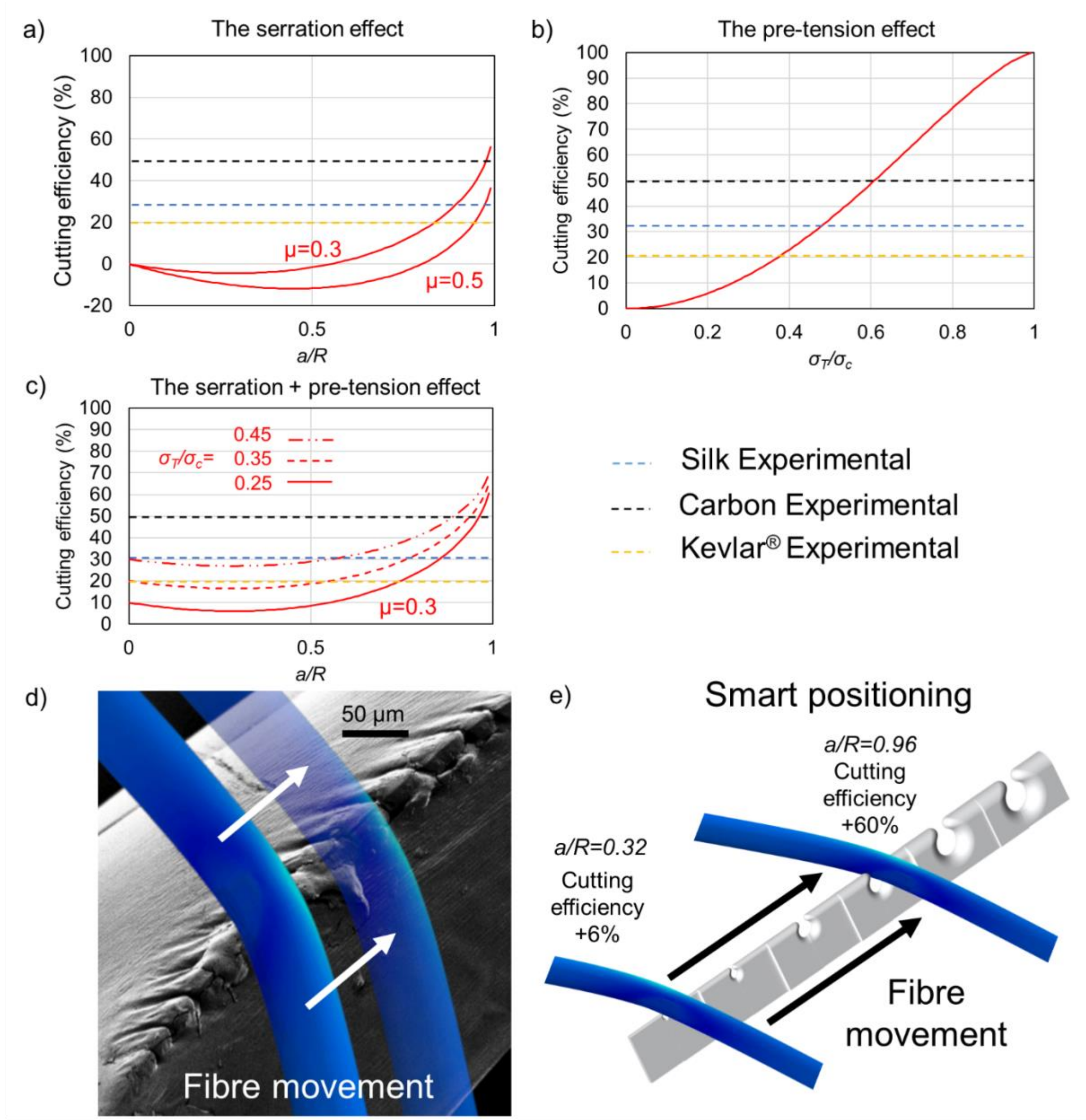

Figure 4. Analytical model of the cutting, smart positioning and optimal cutting. a) Serration effect: Plot of the cutting efficiency vs the *a/R* ratio at two different friction coefficients. b) Pre-tension effect: Plot of the cutting efficiency vs relative pre-tension stress applied by the spider for the different fibre materials. c) Serration + pre-tension effect: Plot of the cutting efficiency vs the *a/R* ratio at different relative pre-tension stresses, showing the effect of both the different serrations and pre-tension stresses. Dashed coloured (blue, black, and yellow) lines indicate the experimental values of the cutting efficiency for the different materials (silk, carbon fibre, and Kevlar® respectively). d) In this panel we propose a schematic of the cutting mechanism: the fibre slides along the serrated edge (SEM image of the real serration) till e) its smart positioning, interlocking in the serration where the cutting is more advantageous. Panel e) values were obtained for $\mu=0.3$ and $\sigma_T/\sigma_c=0.25$. The experimental data are those related to the load necessary to break the fibres obtained from Tables S6, S9, and S12.